PROCEEDINGS OF SCIENCE

New physics in $B \to K^{(*)}$ + invisible

German Valencia*

School of Physics and Astronomy, Monash University,
Wellington Road, Clayton, VIC-3800, Australia

E-mail: german.valencia@monash.edu

We discuss the modes $B \to K^{(*)}$ + invisible in the context of non-standard neutrino interactions as well as in the presence of new light (dark matter) particle pairs. We study models and parameters that can account for the recently reported excess over the SM by Belle II, and consider their implications for additional B decay modes and other phenomenology.

Proceedings of the Corfu Summer Institute 2024 "School and Workshops on Elementary Particle Physics and Gravity" (CORFU2024) 12 - 26 May, and 25 August - 27 September, 2024
Corfu, Greece

*Speaker

PoS(CORFU2024)089

1. Introduction

Rare meson decays into neutrino pairs, such as $B \to K\nu\bar{\nu}$ or $K \to \pi\nu\bar{\nu}$ are theoretically very clean and have long been seen as ideal for precise measurements of SM parameters. Alternatively, they constitute clean windows to new physics. Recently, the Belle II collaboration reported a measurement[1],

$$\mathcal{B}(B^+ \to K^+\nu\bar{\nu})_{\mathtt{exp}} = (2.3 \pm 0.7) \times 10^{-5}, \tag{1}$$

compatible with the SM at the $2.7\,\sigma$ level but still allowing NP contributions six times as large as the SM. This has motivated a renewed interest in studying potential BSM contributions to this mode [2–20]. When the new measurement is averaged with previous ones, the result $\mathcal{B}(B^+ \to K^+\nu\bar{\nu})^{\mathtt{ave}}_{\mathtt{exp}} = (1.3 \pm 0.4) \times 10^{-5}$ [1] is slightly closer to the SM expectation [21],[1]

$$\mathcal{B}(B^+ \to K^+\nu\bar{\nu})_{\mathtt{SM}} = (4.43 \pm 0.31) \times 10^{-6}. \tag{2}$$

For our study, we work with a NP window based on the ratio,

$$R^K_{\nu\nu} \equiv \frac{\mathcal{B}(B^+ \to K^+\nu\bar{\nu})}{\mathcal{B}(B^+ \to K^+\nu\bar{\nu})_{\mathtt{SM}}} \to \begin{cases} (R^K_{\nu\nu})_{\text{new BelleII}} = & 5.3 \pm 1.7, \\ (R^K_{\nu\nu})_{\text{new average}} = & 3.0 \pm 1.0. \end{cases} \tag{3}$$

Numerically, we use both the new Belle II measurement ("new $1\,\sigma$ range") and the new average.

The rates for the charged and neutral B meson decay to a kaon and missing energy are the same without isospin breaking (this happens in both the SM and all the extensions we study), and the measurement of the neutral mode is at present less restrictive so it is not necessary to include it. On the other hand, we need to ensure that any NP satisfies the existing bounds for the related decays into K^*,

$$R^{\nu\nu}_{K^*} = \frac{\mathcal{B}(B \to K^*\nu\bar{\nu})}{\mathcal{B}(B \to K^*\nu\bar{\nu})_{\mathtt{SM}}} \leq 2.7 \text{ or } 1.9. \tag{4}$$

The value 2.7 corresponds to the combined charged and neutral modes as quoted by Belle [23], whereas the value 1.9 corresponds to the strongest experimental constraint from just the neutral mode, $\mathcal{B}(B^0 \to K^{0*}\nu\bar{\nu}) \leq 1.8 \times 10^{-5}$ (90% c.l.) [23].

2. New physics scenarios with neutrinos

In Figure 1, we depict the type of NP we discuss: the diagram on the left for a LEFT description of models with two invisible particles that can be neutrinos or new light dark scalars. This can be realised in models with s-channel mediators (such as a Z') or with t-channel mediators (such as leptoquarks for the neutrino case [3] or vector-like quarks for new invisible scalars [14]). Introduction of mediators permits us to consider additional phenomenological constraints, such as from meson mixing.

[1] This is the result *without* the so-called tree-level contribution, it is a bit lower than the one quoted in [1] due to the use of different CKM parameters, illustrating that there is still some parametric uncertainty [22].

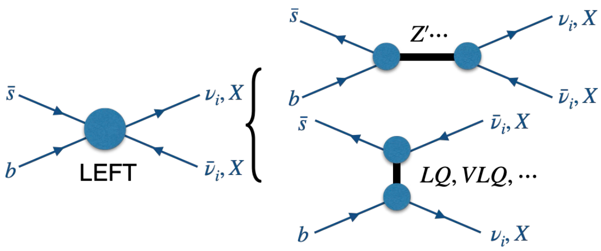

Figure 1: Schematic depiction of interactions in a low-energy effective theory (LEFT) with either neutrinos or new light dark particles in the final state (left) and possible s/t-channel mediators from UV complete models.

We first discuss the case when the invisible particles are neutrinos via the effective Hamiltonian

$$\mathcal{H}_{\rm NP} = -\frac{4G_F}{\sqrt{2}} V_{tb} V_{ts}^{\star} \frac{e^2}{16\pi^2} \sum_{ij} \left(C_L^{ij} O_L^{ij} + C_R^{ij} O_R^{ij} + C_L'^{\,ij} O_L'^{\,ij} + C_R'^{\,ij} O_R'^{\,ij} \right) + \text{ h.c.}, \tag{5}$$

with operators

$$O_L^{ij} = (\bar{s}_L \gamma_\mu b_L)(\bar{\nu}_i \gamma^\mu (1-\gamma_5) \nu_j), \qquad O_R^{ij} = (\bar{s}_R \gamma_\mu b_R)(\bar{\nu}_i \gamma^\mu (1-\gamma_5) \nu_j), \tag{6a}$$

$$O_L'^{\,ij} = (\bar{s}_L \gamma_\mu b_L)(\bar{\nu}_i \gamma^\mu (1+\gamma_5) \nu_j), \qquad O_R'^{\,ij} = (\bar{s}_R \gamma_\mu b_R)(\bar{\nu}_i \gamma^\mu (1+\gamma_5) \nu_j)\ . \tag{6b}$$

The Wilson coefficients in 6 are defined to contain only NP contributions.[2] The operators $O^{ij}_{L,R}$ appear in many standard extensions of the SM, such as through lepto-quark exchange, as we discuss below. In contrast, the operators $O'^{\,ij}_{L,R}$ require light right-handed neutrinos.

2.1 Constraints from $R_K^{\nu\nu}$, $R_{K*}^{\nu\nu}$

Contributions from Eq. 5 to $B \to K^{(*)}\nu\bar{\nu}$ may interfere with the SM, $O^{ii}_{L,R}$, or not, $O^{i\neq j}_{L,R}$ and $O'^{\,ij}_{L,R}$. For $B \to K\nu\bar{\nu}$, only the vector current appears in the hadronic matrix elements, so O_L^{ij} and O_R^{ij} (or $O_L'^{\,ij}$ and $O_R'^{\,ij}$) contribute equally to the rate. For $B \to K^*\nu\bar{\nu}$, both the vector and axial-vector currents play a role. The different neutrino chirality eliminates interference between the contributions from primed and unprimed operators for massless neutrinos. We find numerically [3] using `flavio` [26],[3]

$$R_K^{\nu\nu} \approx 1 - 0.1 \text{ Re} \sum_i (C_L^{ii} + C_R^{ii}) + 0.008 \sum_{ij} \left(\left| C_L^{ij} + C_R^{ij} \right|^2 + \left| C_L'^{\,ij} + C_R'^{\,ij} \right|^2 \right), \tag{7}$$

$$\begin{aligned} R_{K^*}^{\nu\nu} \approx{}& 1 + \text{Re} \sum_i \left(-0.1\, C_L^{ii} + 0.07\, C_R^{ii}\right) \\ &+ \sum_{ij} \left[0.008 \left(|C_L^{ij}|^2 + |C_R^{ij}|^2 + |C_L'^{\,ij}|^2 + |C_R'^{\,ij}|^2 \right) - 0.01 \text{Re} \left(C_L^{ij} C_R^{*ij} + C_L'^{\,ij} C_R'^{*\,ij} \right) \right]. \end{aligned} \tag{8}$$

A few items to note in these equations,

- None of the operators in 6 breaks isospin, so they result in equal rates for the charged and neutral modes.

[2] For comparison, the SM contributes only to C_L^{ii} with value $C_{L\ \rm SM} = -X(x_t)/s_W^2$, $\quad X(x_t) = 1.469 \pm 0.017$ [24, 25].
[3] Analytic expressions can also be found in [27].

- The primed coefficients do not interfere with the SM or with the unprimed ones.
- Several specific cases result in $R_K^{\nu\nu} = R_{K*}^{\nu\nu}$, for example, in models that only produce C_L terms.

2.2 t-channel mediators: leptoquarks

As an example of a t-channel mediator, we use scalar or vector leptoquarks with SM couplings to neutrinos. There are six possibilities

$$\mathcal{L}_S = \lambda_{LS_0}\bar{q}_L^c i\tau_2 \ell_L {S_0}^\dagger + \lambda_{L\tilde{S}_{1/2}}\bar{d}_R\ell_L\tilde{S}_{1/2}^\dagger + \lambda_{LS_1}\bar{q}_L^c i\tau_2\vec{\tau}\cdot\vec{S}_1^\dagger\ell_L + \text{ h. c.} \tag{9}$$
$$\mathcal{L}_V = \lambda_{LV_{1/2}}\bar{d}_R^c\gamma_\mu\ell_L V_{1/2}^{\dagger\mu} + \lambda_{LV_1}\bar{q}_L\gamma_\mu\vec{\tau}\cdot\vec{V}_1^{\dagger\mu}\ell_L + \text{ h. c.,}$$

with different constraints due to correlations with charged lepton modes. These correlations can be written in terms of the usual dimension six operators for that case $O_{9^{(\prime)}}^{ij} = (\bar{s}_{L(R)},\gamma_\mu b_{L(R)})(\bar{\ell}_i\gamma^\mu\ell_j)$, $O_{10^{(\prime)}}^{ij} = (\bar{s}_{L(R)},\gamma_\mu b_{L(R)})(\bar{\ell}_i\gamma^\mu\gamma_5\ell_j)$, and are given by

$$\begin{aligned}
S_0^\dagger : (\bar{3},1,1/3) &\implies C_L^{ij} \\
\tilde{S}_{1/2}^\dagger : (3,2,1/6) &\implies C_{9'}^{ij} = -C_{10'}^{ij} = 2C_R^{ij} \\
\vec{S}_1^\dagger : (\bar{3},3,1/3) &\implies C_9^{ij} = -C_{10}^{ij} = 2C_L^{ij} \\
V_{1/2}^\dagger : (\bar{3},2,5/6) &\implies C_{9'}^{ij} = -C_{10'}^{ij} = 2C_R^{ij} \\
\vec{V}_1^\dagger : (3,3,2/3) &\implies C_9^{ij} = -C_{10}^{ij} = \frac{1}{2}C_L^{ij}
\end{aligned} \tag{10}$$

The contributions from each LQ are

$$C_L^{ij} = \frac{\pi}{\sqrt{2}\alpha G_F V_{td}V_{ts}^*}\left(\frac{\lambda_{LS_0}^{bj}\lambda_{LS_0}^{*si}}{2{m_{S_0}}^2} + \frac{\lambda_{LS_1}^{bj}\lambda_{LS_1}^{*si}}{2{m_{S_1}}^2} - 2\frac{\lambda_{LV_1}^{sj}\lambda_{LV_1}^{*bi}}{{m_{V_1}}^2}\right), \tag{11}$$
$$C_R^{ij} = C_{9'}^{ij} = -C_{10'}^{ij} = \frac{\pi}{\sqrt{2}\alpha G_F V_{td}V_{ts}^*}\left(-\frac{\lambda_{L\tilde{S}_{1/2}}^{sj}\lambda_{L\tilde{S}_{1/2}}^{*bi}}{2m_{\tilde{S}_{1/2}}^2} + \frac{\lambda_{LV_{1/2}}^{bj}\lambda_{LV_{1/2}}^{*si}}{m_{V_{1/2}}^2}\right),$$
$$C_9^{ij} = -C_{10}^{ij} = \frac{\pi}{\sqrt{2}\alpha G_F V_{td}V_{ts}^*}\left(\frac{\lambda_{LS_1}^{bj}\lambda_{LS_1}^{*si}}{{m_{S_1}}^2} - \frac{\lambda_{LV_1}^{sj}\lambda_{LV_1}^{*bi}}{{m_{V_1}}^2}\right).$$

From Eq. 11 we see that taking one LQ at a time results in S_0, S_1, V_1 generating only C_L and thus predicting $R_K^{\nu\nu} = R_{K*}^{\nu\nu}$. This prediction also holds for $S_{1/2}, V_{1/2}$ with *only lepton-flavour diagonal terms*. A scan of the $C_L^{ij} - C_R^{ij}$ ($C_L'^{\,ij}$, $C_R'^{\,ij}$) parameter space is shown in the left panel of Figure 2 as the light (dark) grey region marking the predictions for $R_{K^{(*)}}^{\nu\nu}$ that can be reached from this parameter space. The figure also shows horizontal dashed red lines indicating the two possible numbers for the upper limit $R_{K^*}^{\nu\nu}$ from Eq. 4, as well as vertical solid (dashed) lines marking the current average and new 1σ ranges of Eq. 1. The green area is the 3σ SM prediction. We can see how the prediction $R_K^{\nu\nu} = R_{K*}^{\nu\nu}$ conflicts with the new 1σ range and is only marginally acceptable for the new average, making S_0, S_1, V_1 less appealing.

On the centre panel, we scan over the six parameters in C_R^{ij}, showing that $S_{1/2}, V_{1/2}$ are more promising candidates to explain the excess. We have highlighted in blue (red) the regions that satisfy the new Belle II measurement and $R_{K^*}^{\nu\nu} \leq 2.7$ (1.9) to correlate them with predictions for other modes. Finally, the right panel repeats this scan, fixing $C_R^{ee} = C_R^{\mu\mu} = 0$ as discussed below.

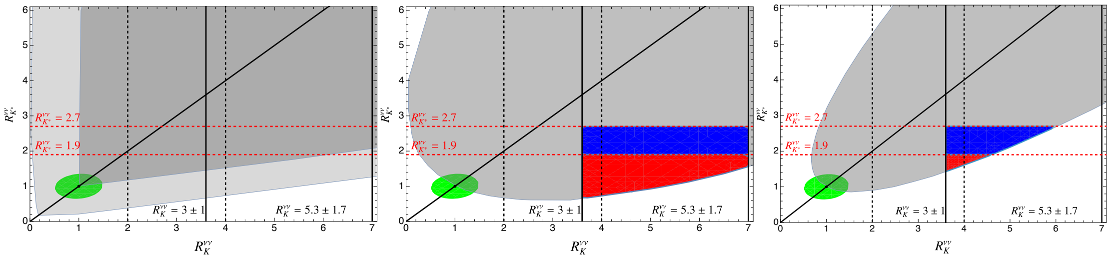

Figure 2: The correlation between $R_K^{\nu\nu}$ and $R_{K^*}^{\nu\nu}$ obtained by scanning the 12 parameters C_L^{ij}, C_R^{ij} is shown in light grey, while that for $C_L'^{\,ij}, C_R'^{\,ij}$ is shown in dark grey (left panel). We also highlight the $3\,\sigma$ SM prediction in green. The centre panel shows the scan of the 6 parameters in C_R^{ij}, whereas the right panel only scans 4 parameters from C_R^{ij}, taking $C_R^{\mu\mu} = C_R^{ee} = 0$. The points highlighted in blue or red fall within the new 1σ range of $R_K^{\nu\nu}$ (also marked by the vertical solid black lines). Additionally, the blue (red) points satisfy $R_{K^*}^{\nu\nu} \leq 2.7$ (1.9) respectively (values marked by the horizontal dashed red lines). The diagonal black line is $R_K = R_{K^*}$.

2.3 Correlations with charged lepton modes

S_0 also modifies $R_D^{(*)}$ as it induces the operator $\bar{c}b\bar{\tau}\nu^i$. Defining $r_{D^{(*)}} = \frac{R_{D^{(*)}}}{R_{D^{(*)}\,SM}}$, we find

$$r_D = r_{D^*} = \left(\frac{\alpha}{2\pi}\right)^2 | \left(C_L^{3,1}|^2 + |C_L^{3,2}|^2\right) + |1 - \frac{\alpha}{2\pi} C_L^{3,3}|^2. \tag{12}$$

The HFLAV numbers from Moriond 2024 [28] are $r_D = 1.15 \pm 0.09$, $r_{D^*} = 1.13 \pm 0.05$. On the other hand, if we take a high value $R_K^{\nu\nu} = R_{K*}^{\nu\nu} \sim 3.5$, we can only reach $r_{D^{(*)}} \lesssim 1.06$, so that the two observables are in conflict [27], making S_0 a less attractive option.

Recent global fits to $b \to s\ell^+\ell^-$ processes suggest that $|C_9^{\mu\mu}| \sim |C_9^{ee}| \lesssim 1$, with C_{10} being somewhat smaller for both muons and electrons. The correlations implied by S_1 or V_1 Eq. 11 then imply minimal effect from lepton flavour diagonal terms $C_L^{ee,\mu\mu}$ for $R_K^{\nu\nu}$, $R_{K*}^{\nu\nu}$.

A visualisation of the parameter space [29–31] that can be seen here indicates that at least one of the diagonal entries, C_R^{ii}, needs to be large, around ten, to find a solution. This conflicts with $b \to s\ell^+\ell^-$ results for both C_R^{ee} and $C_R^{\mu\mu}$, leading us to conclude that the only possibility is that $C_R^{\tau\tau}$ is large. This motivates the separate scan shown on the right panel of Figure 2.

The preferred parameter regions in this case (red and blue) lead to predictions of large enhancements over the SM in the rates for $B_s \to \tau\tau$ and $B^+ \to K^+\tau\tau$, illustrated in Figure 3. These regions also lead to large charged lepton flavour violation in $B_s \to \tau^+\mu^-$ and $B^+ \to K^+\tau^+\mu^-$ shown in the same Figure. In this regard, it is interesting to note that the current upper bound on the C_R^{ij} coefficients from CLFV processes is less restrictive than what results from $R_K^{\nu\nu}$ except for μe flavours. This comparison, for one LQ at a time is shown in Table 1 [3].

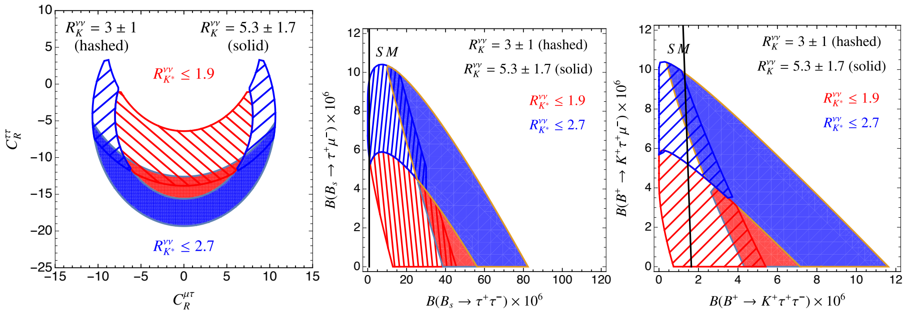

Figure 3: The left panel shows the allowed region in $C_R^{\tau\tau} - C_R^{\mu\tau}$ satisfying $R^{\nu\nu}_{K^{(*)}}$ as per Eqs. 3-4, with the same colour coding of previous figures. A map of these regions onto predictions for other B meson decay modes is shown in the other two panels. The solid black line for the lepton flavour conserving processes marks the SM prediction.

LQ	upper bound on $C^{ij}_{L,R}$ from CLFV B decays			from $R^\nu_K = R^\nu_{K^*} \lesssim 2$		
				$ij = \mu e$	$ij = e\tau$	$ij = \mu\tau$
$\tilde{S}_{1/2}$	$\lvert C_R^{\mu e}\rvert \lesssim 0.4$	$\lvert C_R^{e\tau}\rvert \lesssim 26$	$\lvert C_R^{\mu\tau}\rvert \lesssim 35$	1.001	6.4	11
S_1	$\lvert C_L^{\mu e}\rvert \lesssim 0.2$	$\lvert C_L^{e\tau}\rvert \lesssim 13$	$\lvert C_L^{\mu\tau}\rvert \lesssim 18$	1.0003	2.4	3.5
$V_{1/2}$	$\lvert C_R^{\mu e}\rvert \lesssim 0.4$	$\lvert C_R^{e\tau}\rvert \lesssim 26$	$\lvert C_R^{\mu\tau}\rvert \lesssim 35$	1.001	6.4	11
$V_1^\dagger$	$\lvert C_L^{\mu e}\rvert \lesssim 0.8$	$\lvert C_L^{e\tau}\rvert \lesssim 52$	$\lvert C_L^{\mu\tau}\rvert \lesssim 70$	1.005	23	40

Table 1: Upper bound on coefficients $C^{ij}_{L,R}$ taken one at a time from constraints on charged lepton flavour violating modes [3] compared with the corresponding constraints from $R^\nu_K = R^\nu_{K^*} \lesssim 2$ for different leptoquarks.

2.4 s-channel Z' mediators

We can generate the operators $C'^{ij}_{L,R}$ in Eq. 6 in models with new light sterile neutrinos. A scan of the relevant parameter space is shown in the left panel of Figure 2 as the dark grey region. The region is smaller than what can be covered with the $C^{ij}_{L,R}$ coefficients, and the rates are always larger than the SM rates, because there is no interference with the SM. A specific model where the right-handed neutrino couples to the SM fields via a Z' mediator runs into trouble satisfying the constraint imposed by B mixing. This constraint implies that only the $R^{\nu\nu}_K \approx R^{\nu\nu}_{K^*} \lesssim 2$ is accessible [3, 32, 33], and is thus not a good candidate to explain an excess in $B^+ \to K^+ +$ missing E as the one implied by the Belle II number.

3. New light invisible particles

The Belle II measurement also provides a window into new invisible light particles, with masses $m < m_B - m_K$. Here, we assume that they must be pair-produced due to a $\mathbb{Z}_2$ symmetry or a dark charge so that they result in a three-body decay. We have considered the spin cases 0, 1/2, and 1 in [5, 27], but will discuss only the scalar case in this talk. We assume that mediators occur at a high scale and can be integrated out to produce an effective ϕLEFT.

3.1 ϕLEFT

With scalar invisible particles, there are only two operators up to dimension six that contribute to $B^+ \to K^+ +$ missing E,

$$\mathcal{L} = \frac{1}{\Lambda_{\rm eff}} O^{S,sb}_{q\phi} + \frac{1}{\Lambda^2_{\rm eff}} O^{V,sb}_{q\phi} \tag{13}$$
$$O^{S,sb}_{q\phi} = (\bar{s}b)(\phi^\dagger\phi), \quad O^{V,sb}_{q\phi} = (\bar{s}\gamma^\mu b)(\phi^\dagger i \overleftrightarrow{\partial_\mu} \phi),$$

and the second one (in blue) vanishes for real scalars. In an effective theory at the electroweak scale, ΦSMEFT, they both arise at dimension six as the first one may look like

$$\frac{1}{\Lambda_{\rm eff}} O^{S,sb}_{q\phi} \in \frac{v}{\Lambda^2_{\rm eff}} (\bar{q}_{2L} b_R H)(\phi^\dagger\phi) \tag{14}$$

The parameter space allowed by current data is shown in Figure 4. One can further discriminate between models by comparing the spectrum shape. This is illustrated on the right panel of the same figure, following [27] but emphasising that not enough information has been released by the Belle II collaboration for a definitive comparison with the spectrum. In any case, since the current result suggests that the enhancement is due to the region $3 \le q^2 \le 7$ GeV^2, the figure indicates that if the new physics has coupling $O^{S,sb}_{q\phi}$ the data would prefer $m_\phi \sim 300$ MeV.

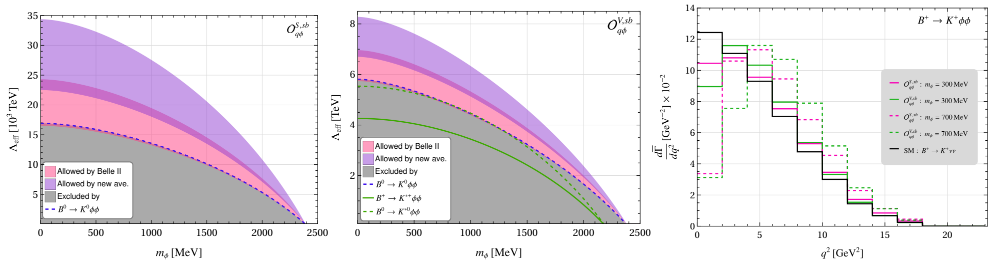

Figure 4: Left and centre panels: the parameter space that could explain the recent Belle II excess [new average] is shown in pink [purple] with scalar DM for scalar (vector) quark current operators $O^{S,sb}_{q\phi}$-left panel ($O^{V,sb}_{q\phi}$ - centre panel). The grey region is excluded by other B meson decay modes that are indicated in the plots by coloured lines. The right panel shows the q^2 distribution of normalised differential decay widths after taking into account the experimental efficiency.

3.2 Mediators and dark matter

We turn to the questions of possible mediators to generate the ϕLEFT operators in a UV complete theory and to whether the new scalars can be identified with dark matter candidates. The importance of the first question was already illustrated above for right-handed neutrinos. Whereas the effective theory was a plausible candidate to explain an excess, a Z' mediator is ruled it out due to additional constraints. Following that example, and referring to Figure 1, we can guess that t-channel mediators will have an easier time satisfying B mixing constraints than s-channel mediators. With this in mind, we construct an explicit model with t-channel vector-like quark mediators [14].

PoS(CORFU2024)089

The basic ingredients of the model are two heavy vector-like quarks $Q \sim (\mathbf{3}, \mathbf{2}, 1/6)$, $D \sim (\mathbf{3}, \mathbf{1}, -1/3)$ and a light scalar field $\phi \sim (\mathbf{1}, \mathbf{1}, 0)$. All the new fields are odd under a $\mathbb{Z}_2$ symmetry to stabilise the dark matter particle ϕ. These are the conditions that produce $O^{S,sb}_{q\phi}$ in ϕLEFT framework above. The Lagrangian for our model is

$$\mathcal{L}^{\rm NP}_{\tt kinetic} = \bar{Q} i \not{D} Q - m_Q \bar{Q} Q + \bar{D} i \not{D} D - m_D \bar{D} D + \frac{1}{2}\partial_\mu \phi \partial^\mu \phi - \frac{1}{2} m_\phi^2 \phi^2, \tag{15}$$

$$\mathcal{L}^{\rm NP}_{\tt Yukawa} = y_q^p \bar{q}_{Lp} Q_R \phi + y_d^p \bar{D}_L d_{Rp} \phi - y_1 \bar{Q}_L D_R H - y_2 \bar{Q}_R D_L H + \text{h.c.}\,, \tag{16}$$

$$V^{\rm NP}_{\tt potential} = \frac{1}{4}\lambda_\phi \phi^4 + \frac{1}{2}\kappa\, \phi^2 H^\dagger H\,, \tag{17}$$

At low energy, after integrating out the heavy vector-like quarks, this leads to

$$\mathcal{L}^{\rm LEFT}_{\phi\phi qq} = \frac{1}{2} C^{S,ij}_{d\phi} (\bar{d}_i d_j)\phi^2 + \frac{1}{2} C^{P,ij}_{d\phi} (\bar{d}_i i\gamma_5 d_j)\phi^2 + \frac{1}{2} C^{S,ij}_{u\phi} (\bar{u}_i u_j)\phi^2 + \frac{1}{2} C^{P,ij}_{u\phi} (\bar{u}_i i\gamma_5 u_j)\phi^2 \tag{18}$$

$$C^{S,ij}_{d\phi} = \frac{(y_q^i y_d^j y_1 + y_q^{j*} y_d^{i*} y_1^*) v}{\sqrt{2} m_Q m_D} + \left(\frac{y_q^i y_q^{j*}}{2m_Q^2} + \frac{y_d^{i*} y_d^j}{2m_D^2} \right) (m_{d_i} + m_{d_j})$$

$$i C^{P,ij}_{d\phi} = \frac{(y_q^i y_d^j y_1 - y_q^{j*} y_d^{i*} y_1^*) v}{\sqrt{2} m_Q m_D} - \left(\frac{y_q^i y_q^{j*}}{2m_Q^2} - \frac{y_d^{i*} y_d^j}{2m_D^2} \right) (m_{d_i} - m_{d_j}),$$

$$C^{S,ij}_{u\phi} = \frac{\tilde{y}_q^i \tilde{y}_q^{j*}}{2m_Q^2} (m_{u_i} + m_{u_j}), \quad i C^{P,ij}_{u\phi} = -\frac{\tilde{y}_q^i \tilde{y}_q^{j*}}{2m_Q^2} (m_{u_i} - m_{u_j})\,, \tag{19}$$

The model is then a candidate to explain the possible Belle II excess, for example, with $C^{S,sb}_{d\phi} \sim (3-8)/(10^5\ \text{TeV})$ and $m_\phi = 1$ GeV as can be seen in Figure 5

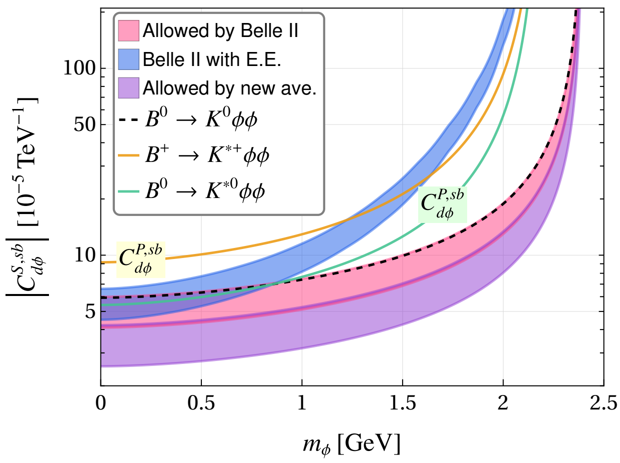

Figure 5: Preferred parameter space to accommodate the $B^+ \to K^+$ + inv measurements with decaysinto DM final states, $B^+ \to K^+\phi\phi$: latest Belle II measurement [1] in red, reweighted to account for the selection efficiency in blue; using the new average in purple [1]. The dashed line indicates the current constraint from $B^0 \to K^0$ + inv [23, 34] on $|C^{S,sb}_{d\phi}|$ and the solid orange and green lines the constraints on $|C^{P,sb}_{d\phi}|$ posed by the searches for $B^+ \to K^{+*}$ + inv and $B^0 \to K^{0*}$ + inv [23, 34], respectively.

3.3 Identifying the ϕ scalar as a dark matter candidate

To investigate whether this is possible, we require two conditions

- Calculating the dark-matter annihilation cross-section, we check that it is possible to produce the correct relic density $\Omega\hbar^2 = 0.12$ through the thermal freeze-out mechanism. For this kinematic regime, the possible annihilation channels are into pions, kaons and etas, so we rely on a chiral realisation of Eq. 18.

  To achieve this we need the thermally averaged cross-section to be $\langle\sigma v\rangle \simeq 2.4\times10^{-26}\,\frac{\mathrm{cm}^3\mathrm{s}^{-1}}{(\hbar c)^2 c} = 2.2\times10^{-9}\,\mathrm{GeV}^{-2}$ [35], which implies that we need $C^{S,ss}_{d\phi} \sim (0.1)/(\mathrm{TeV})$.

- We also need to avoid direct detection constraints, in particular those using the Migdal effect for sub-GEV dark matter [36–38] as reported by the liquid xenon and argon experiments, including XENON1T [39], DarkSide50 [40], LZ [41], and PandaX-4T [42]. We follow [43] to calculate the effective DM-nucleon cross section.

- To produce the correct relic density and an excess in $B \to K^{(*)}$ + invisible compatible with the Belle II observation, we only need the coefficients $C^{S,sb}_{d\phi}$ and $C^{S,ss}_{d\phi}$ but this scenario is already ruled out by Panda X4T as seen in the left pane of Figure 6.

  Viable models require an interplay between different parameters. One example that satisfies all the conditions is shown in the right panel of Figure 6, corresponding to the choice $|y^d_{q,d}| \sim 0.2|y^s_{q,d}|$, which leads to $|C^{S,dd}_{d\phi}| \sim 0.2|C^{S,ds}_{d\phi}| \sim 0.04|C^{S,ss}_{d\phi}|$.

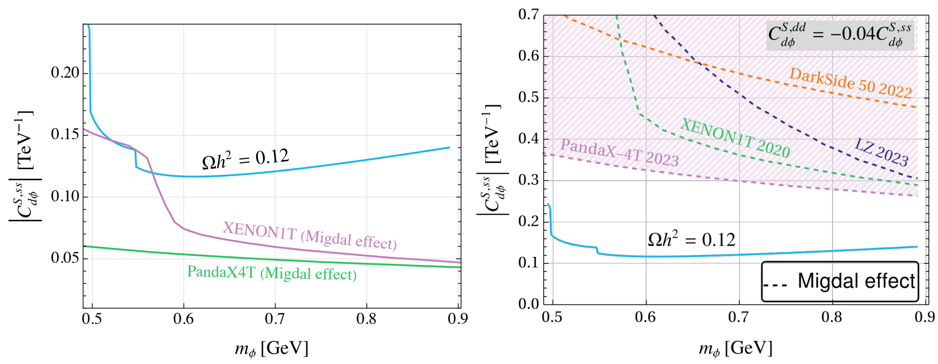

Figure 6: Value of $C^{S,ss}_{d\phi}$ needed to produce the correct relic density for different scalar masses (left). To also satisfy direct detection constraints from the Migdal effect, additional parameters are needed; the right panel shows the situation with $|C^{S,dd}_{d\phi}| \sim 0.04|C^{S,ss}_{d\phi}|$

For this choice of parameters, we have checked that other phenomenological constraints are also satisfied, $gg \to H$, $H \to \gamma\gamma$, $B_s \to \phi\phi$, B_s, B_d and K mixing, $B \to X_s\gamma$ and $D \to \phi\phi$ [14].

The effective interactions of Eq. 14 can motivate different UV completions with interesting phenomenology. For example, a 2HDM plus scalar dark matter completion [20] has sources of CP violation in $\Delta S = 1$ transitions that go beyond what can be probed by ϵ and ϵ' and can lead to large CP-violating asymmetries in hyperon decay. Recall that are the two CP violating parameters extracted from $K \to \pi\pi$ amplitudes as [44]

$$\eta^{+-} = \frac{A(K_L \to \pi^+\pi^-)}{A(K_S \to \pi^+\pi^-)} = \epsilon + \epsilon', \qquad \eta^{00} = \frac{A(K_L \to \pi^0\pi^0)}{A(K_S \to \pi^0\pi^0)} = \epsilon - 2\epsilon' \tag{20}$$

Their measured values agree with the SM but the calculations still suffer from large uncertainties [45, 46], leaving some room for new physics contributions. Another direction in NP parameter space is probed by asymmetries in hyperon non-leptonic decay, such as

$$A^{\Lambda}_{CP} = \frac{\alpha + \overline{\alpha}}{\alpha - \overline{\alpha}} \tag{21}$$

$$\frac{d\Gamma(\Lambda \to p\pi^-)}{d\Omega} \sim \left(1 + \alpha\, \mathcal{P}_\Lambda \cdot \hat{\mathbf{p}}_p\right), \tag{22}$$

where α measures the correlation between the Λ polarisation and the proton momentum, and $\bar{\alpha}$ the corresponding parameter for $\bar{\Lambda}$ decay. We illustrate this in Figure 7, where the size of the CP asymmetry in $\Lambda \to p\pi^-$ decay, A^{Λ}_{CP}, is shown as a function of the three main observables that constrain it: kaon mixing, direct and indirect CP violation in kaon decay. It can reach levels within the sensitivity of BES III.

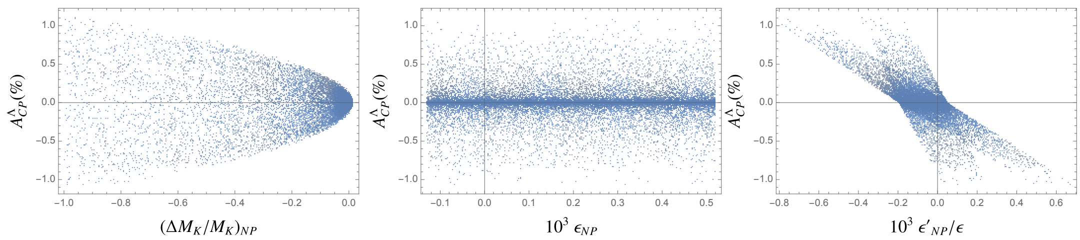

Figure 7: Distributions of $A^{\Lambda,\text{new}}_{CP}$ versus $\Delta M_K^{\text{new}}/\Delta M_K^{\text{exp}}$ (left), ε_{new} (centre), and $\varepsilon'_{\text{new}}/\varepsilon$ (right), in the 2HDM plus light scalar model of [20].

4. Summary and conclusions

Motivated by the recent Belle II result, we explored the NP physics window that could enhance the mode $B^+ \to K^+ + \texttt{invisible}$ over the SM $B^+ \to K^+\nu\bar{\nu}$. At the same time, we require consistency with the existing 90% c.l upper bounds on the related modes $B \to K^{(*)}\nu\bar{\nu}$ and $B^0 \to K^0\nu\bar{\nu}$. We also consider correlations with charged lepton modes.

We find that neutrino LFV couplings, with only left-handed neutrinos, can reproduce the rates for these modes,

- When induced by a single LQ exchange, $S_{1/2}, V_{1/2}$ can reproduce the rates provided at least one of the lepton flavour diagonal coefficients is of order 10.
- Measurements of $b \to s\ell^+\ell^-$ processes rule out this possibility for dielectron and dimuon modes, leaving the ditau modes as the only option.
- This solution then predicts enhancements in rare B decays with ditau final states and also large charged lepton flavour violating modes with muon-tau.

The invisible particle can also be pairs of new scalars, vectors or fermions. We constructed the lowest dimensionality ϕLEFT for these cases, selecting only operators relevant for these modes. There are viable regions of parameter space for several of these operators that can explain the excess in $B^+ \to K^+ +$ `invisible`. Future measurements of the missing energy spectrum can discriminate between some of these possibilities.

We presented an explicit t-channel mediated model involving two vector-like quarks to illustrate that a pair of light scalars enhancing $B^+ \to K^+ +$ `invisible` is consistent with these scalars being dark matter particles in the sense that their annihilation can produce the correct relic density and that the parameter space allow you to evade direct detection constraints including the Migdal effect.

We commented on other possible UV completions and their interesting effects on CP violating observables.

Acknowledgments

This work was supported in part by the Australian Government through the Australian Research Council. This talk was based on work done in collaboration with Xiao-Gang He, Xiao-Dong Ma, Michael Schmidt, Raymond Volkas and Jusak Tandean.

References

[1] Belle-II collaboration, I. Adachi et al., *Evidence for $B^+ \to K^+ \nu\bar{\nu}$ Decays*, 2311.14647.

[2] C. Bird, P. Jackson, R. V. Kowalewski and M. Pospelov, *Search for dark matter in $b \to s$ transitions with missing energy* , *Phys. Rev. Lett.* **93** (2004) 201803, [hep-ph/0401195].

[3] X. G. He and G. Valencia, *RK(∗)ν and non-standard neutrino interactions*, *Phys. Lett. B* **821** (2021) 136607, [2108.05033].

[4] T. Felkl, S. L. Li and M. A. Schmidt, *A tale of invisibility: constraints on new physics in $b \to s\nu\nu$*, *JHEP* **12** (2021) 118, [2111.04327].

[5] X.-G. He, X.-D. Ma and G. Valencia, *FCNC B and K meson decays with light bosonic Dark Matter*, *JHEP* **03** (2023) 037, [2209.05223].

[6] P. Asadi, A. Bhattacharya, K. Fraser, S. Homiller and A. Parikh, *Wrinkles in the Froggatt-Nielsen Mechanism and Flavorful New Physics*, 2308.01340.

[7] R. Bause, H. Gisbert and G. Hiller, *Implications of an enhanced $B \to K\nu\bar{\nu}$ branching ratio*, 2309.00075.

[8] L. Allwicher, D. Becirevic, G. Piazza, S. Rosauro-Alcaraz and O. Sumensari, *Understanding the first measurement of $\mathcal{B}(B \to K\nu\bar{\nu})$*, 2309.02246.

[9] P. Athron, R. Martinez and C. Sierra, *B meson anomalies and large $B^+ \to K^+\nu\bar{\nu}$ in non-universal $U(1)'$ models*, 2308.13426.

[10] T. Felkl, A. Giri, R. Mohanta and M. A. Schmidt, *When Energy Goes Missing: New Physics in $b \to s\nu\nu$ with Sterile Neutrinos*, 2309.02940.

[11] M. Abdughani and Y. Reyimuaji, *Constraining light dark matter and mediator with $B^+ \to K^+\nu\bar{\nu}$ data*, 2309.03706.

[12] H. K. Dreiner, J. Y. Günther and Z. S. Wang, *The Decay $B \to K\nu\bar{\nu}$ at Belle II and a Massless Bino in R-parity-violating Supersymmetry*, 2309.03727.

[13] M. Ovchynnikov, M. A. Schmidt and T. Schwetz, *Complementarity of $B \to K^{(*)}\mu\bar{\mu}$ and $B \to K^{(*)}$ + inv for searches of GeV-scale Higgs-like scalars*, Eur. Phys. J. C **83** (2023) 791, [2306.09508].

[14] X.-G. He, X.-D. Ma, M. A. Schmidt, G. Valencia and R. R. Volkas, *Scalar dark matter explanation of the excess in the Belle II $B^+ \to K^+$+ invisible measurement*, JHEP **07** (2024) 168, [2403.12485].

[15] C. S. Kim, D. Sahoo and K. N. Vishnudath, *Searching for signatures of new physics in $B \to K\,\nu\,\bar{\nu}$ to distinguish between Dirac and Majorana neutrinos*, Eur. Phys. J. C **84** (2024) 882, [2405.17341].

[16] A. J. Buras, J. Harz and M. A. Mojahed, *Disentangling new physics in $K \to \pi\nu\bar{\nu}$ and $B \to K\,(K^*)\,\nu\bar{\nu}$ observables*, JHEP **10** (2024) 087, [2405.06742].

[17] S. Rosauro-Alcaraz and L. P. S. Leal, *Disentangling left and right-handed neutrino effects in $B \to K^{(*)}\nu\nu$*, Eur. Phys. J. C **84** (2024) 795, [2404.17440].

[18] D. Marzocca, M. Nardecchia, A. Stanzione and C. Toni, *Implications of $B \to K\nu\bar{\nu}$ under rank-one flavor violation hypothesis*, Eur. Phys. J. C **84** (2024) 1217, [2404.06533].

[19] P. D. Bolton, S. Fajfer, J. F. Kamenik and M. Novoa-Brunet, *Signatures of light new particles in B→K(*)Emiss*, Phys. Rev. D **110** (2024) 055001, [2403.13887].

[20] X.-G. He, X.-D. Ma, J. Tandean and G. Valencia, *$B \to K$+invisible, dark matter, and CP violation in hyperon decays*, 2502.09603.

[21] D. Bečirević, G. Piazza and O. Sumensari, *Revisiting $B \to K^{(*)}\nu\bar{\nu}$ decays in the Standard Model and beyond*, Eur. Phys. J. C **83** (2023) 252, [2301.06990].

[22] A. J. Buras, *Standard Model predictions for rare K and B decays without new physics infection*, Eur. Phys. J. C **83** (2023) 66, [2209.03968].

[23] Belle collaboration, J. Grygier et al., *Search for $\boldsymbol{B \to h\nu\bar{\nu}}$ decays with semileptonic tagging at Belle*, Phys. Rev. D **96** (2017) 091101, [1702.03224].

[24] G. Buchalla and A. J. Buras, *The rare decays $K \to \pi\nu\bar{\nu}$, $B \to X\nu\bar{\nu}$ and $B \to l^+l^-$: An Update*, Nucl. Phys. B **548** (1999) 309–327, [hep-ph/9901288].

[25] J. Brod, M. Gorbahn and E. Stamou, *Two-Loop Electroweak Corrections for the $K \to \pi\nu\bar{\nu}$ Decays*, Phys. Rev. D **83** (2011) 034030, [1009.0947].

[26] D. M. Straub, *flavio: a Python package for flavour and precision phenomenology in the Standard Model and beyond*, 1810.08132.

[27] X.-G. He, X.-D. Ma and G. Valencia, *Revisiting models that enhance B+→K+νν ¯ in light of the new Belle II measurement*, Phys. Rev. D **109** (2024) 075019, [2309.12741].

[28] Heavy Flavor Averaging Group (HFLAV) collaboration, S. Banerjee et al., *Averages of b-hadron, c-hadron, and τ-lepton properties as of 2023*, 2411.18639.

[29] U. Laa, D. Cook and G. Valencia, *A slice tour for finding hollowness in high-dimensional data*, Journal of Computational and Graphical Statistics **29** (2020) 681–687, [1910.10854].

[30] U. Laa and G. Valencia, *Pandemonium: a clustering tool to partition parameter space—application to the B anomalies*, Eur. Phys. J. Plus **137** (2022) 145, [2103.07937].

[31] U. Laa, A. Aumann, D. Cook and G. Valencia, *New and Simplified Manual Controls for Projection and Slice Tours, With Application to Exploring Classification Boundaries in High Dimensions*, Journal of Computational and Graphical Statistics **32** (2023) 1229–1236, [https://doi.org/10.1080/10618600.2023.2206459].

[32] X.-G. He and G. Valencia, *B decays with τ leptons in nonuniversal left-right models*, Phys. Rev. D **87** (2013) 014014, [1211.0348].

[33] X.-G. He and G. Valencia, *Lepton universality violation and right-handed currents in $b \to c\tau\nu$*, Phys. Lett. B **779** (2018) 52–57, [1711.09525].

[34] Belle collaboration, O. Lutz et al., *Search for $B \to h^{(*)} \nu\bar{\nu}$ with the full Belle $\Upsilon(4S)$ data sample*, Phys. Rev. D **87** (2013) 111103, [1303.3719].

[35] G. Steigman, B. Dasgupta and J. F. Beacom, *Precise relic WIMP abundance and its impact on searches for dark matter annihilation*, Phys. Rev. D **86** (2012) 023506, [1204.3622].

[36] A. Migdal, *Ionization of atoms accompanying α- and β-decay*, *J. Phys. Acad. Sci. USSR* **4** (1941) 449.

[37] M. Ibe, W. Nakano, Y. Shoji and K. Suzuki, *Migdal effect in dark matter direct detection experiments*, JHEP **03** (2018) 194, [1707.07258].

[38] M. J. Dolan, F. Kahlhoefer and C. McCabe, *Directly detecting sub-GeV dark matter with electrons from nuclear scattering*, Phys. Rev. Lett. **121** (2018) 101801, [1711.09906].

[39] XENON collaboration, E. Aprile et al., *Search for Light Dark Matter Interactions Enhanced by the Migdal Effect or Bremsstrahlung in XENON1T*, Phys. Rev. Lett. **123** (2019) 241803, [1907.12771].

[40] DarkSide collaboration, P. Agnes et al., *Search for Dark-Matter-Nucleon Interactions via Migdal Effect with DarkSide-50*, Phys. Rev. Lett. **130** (2023) 101001, [2207.11967].

[41] LZ collaboration, J. Aalbers et al., *Search for new physics in low-energy electron recoils from the first LZ exposure*, Phys. Rev. D **108** (2023) 072006, [2307.15753].

[42] PandaX collaboration, D. Huang et al., *Search for Dark-Matter-Nucleon Interactions with a Dark Mediator in PandaX-4T*, *Phys. Rev. Lett.* **131** (2023) 191002, [2308.01540].

[43] E. Del Nobile, *The Theory of Direct Dark Matter Detection: A Guide to Computations*, 2104.12785.

[44] Particle Data Group collaboration, S. Navas et al., *Review of particle physics*, *Phys. Rev. D* **110** (2024) 030001.

[45] J. Brod, M. Gorbahn and E. Stamou, *Standard-Model Prediction of* ϵ_K *with Manifest Quark-Mixing Unitarity*, *Phys. Rev. Lett.* **125** (2020) 171803, [1911.06822].

[46] V. Cirigliano, H. Gisbert, A. Pich and A. Rodríguez-Sánchez, *Isospin-violating contributions to* ϵ'/ϵ, *JHEP* **02** (2020) 032, [1911.01359].